Inorganic Chemistry Communications 170 (2024) 113299

Contents lists available at ScienceDirect

Inorganic Chemistry Communications

journal homepage: www.elsevier.com/locate/inoche

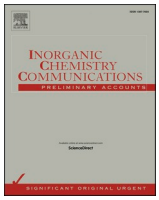

Research Article

Green synthesized Cr_2O_3/Bi_2O_3 nanocomposites for gamma ray shielding

K. Kruthika [a], S.M. Rumana Farheen [a], H.C. Manjunatha [b,*], Y.S. Vidya [c,*], K.N. Sridhar [d], R. Munirathnam [e], S. Manjunatha [d], S. Krishnaveni [a,*]

[a] Department of Studies in Physics, Manasagangotri, University of Mysore, Mysuru 570006, Karnataka, India
[b] Department of Physics, Government First Grade College, Devanahalli 562110, Karnataka, India
[c] Department of Physics, Lal Bahadur Shastri Government First Grade College, Bangalore 560032, Karnataka, India
[d] Department of Physics, Government First Grade College, Maluru 563130, Karnataka, India
[e] Department of Physics, Government College for Women, Kolar 563101, Karnataka, India

ARTICLE INFO

Keywords:
Green synthesis
Cr_2O_3/Bi_2O_3
Radiation shielding
Gamma radiation
NaI(Tl) detector

ABSTRACT

The quest for advanced materials in gamma radiation shielding has spurred the exploration of environmentally friendly, nanotechnology-based approaches. This study introduces a novel synthesis of Cr_2O_3/Bi_2O_3 nanocomposites (NCs) using the solution combustion method, with Aloe vera extract serving as a natural reducing agent. Comprehensive analytical characterization of the synthesized NCs was conducted using powder X-ray diffraction (PXRD), scanning electron microscopy (SEM), energy-dispersive X-ray spectroscopy (EDS), Fourier-transform infrared spectroscopy (FTIR), and ultraviolet–visible (UV–Vis) spectroscopy. The gamma radiation shielding properties of the Cr_2O_3/Bi_2O_3 NCs are evaluated using a NaI(Tl) detector connected to a multichannel analyzer. Key shielding parameters, including mass attenuation coefficients, mean free path, half-value layer, tenth-value layer, energy buildup factor, and radiation protection efficiency, indicate that Cr_2O_3/Bi_2O_3 NCs are highly effective in gamma radiation shielding. The results demonstrated the feasible shielding performance of these nanocomposites across various energies within error limits of 5 %. This study highlights the potential of Cr_2O_3/Bi_2O_3 NCs as a promising, sustainable alternative to conventional shielding materials, offering enhanced gamma radiation protection with reduced environmental impact.

1. Introduction

Effective shielding against gamma radiation is essential to mitigate its harmful effects on human health, ensure safety in radiation-intensive environments, protect sensitive equipment, and minimize environmental contamination [1,2]. When considering gamma shielding, the primary objective is to reduce the intensity of gamma radiation passing through a material [3,4]. This is typically achieved through a combination of factors including the thickness, density, and composition of the shielding material [5]. Conventional gamma shielding materials, such as lead, concrete, and steel, have been widely utilized for their ability to attenuate gamma radiation [6,7]. However, these materials often come with drawbacks such as high weight, bulkiness, and environmental concerns [8,9]. In recent years, there has been growing interest in exploring alternative shielding materials that offer improved efficiency, reduced environmental impact, and greater versatility [10,11].

Nanoparticles, with their unique properties stemming from their small size and high surface area-to-volume ratio, have emerged as promising candidates for gamma shielding applications [12]. Traditional methods of synthesizing nanoparticles often involve chemical processes that may generate hazardous byproducts or require the use of toxic chemicals [13,14]. Green synthesis methods utilize environmentally benign substances such as plant extracts, microorganisms, or environmentally friendly solvents to produce nanoparticles [15,16]. These methods aim to reduce the environmental impact and health risks associated with nanoparticle synthesis. These environmentally friendly NCs hold promise for various applications in nuclear power, medical imaging, space exploration, and other fields where gamma radiation protection is essential.

Chromium (Cr) can be used as a component in composites or coatings for radiation shielding applications [17,18]. The combination of its high density, stability, and compatibility, makes chromium a viable option for gamma radiation shielding in various industrial, medical, and research applications [19–24]. Cr can be easily integrated into various forms of shielding structures, such as sheets, plates, or coatings, making them adaptable to different shielding configurations and environments

* Corresponding authors at: Department of Chemistry, BMS College of Engineering, Bangalore 560019, Karnataka, India.
E-mail addresses: manjunathhc@rediffmail.com (H.C. Manjunatha), vidyays.phy@gmail.com (Y.S. Vidya), sk@physics.uni-mysore.ac.in (S. Krishnaveni).

https://doi.org/10.1016/j.inoche.2024.113299
Received 25 April 2024; Received in revised form 15 September 2024; Accepted 5 October 2024
Available online 11 October 2024

[25–28]. Moreover, Cr is relatively abundant and cost-effective compared to commonly used materials used for gamma shielding, such as lead [29,30]. This makes it an attractive option for applications where cost considerations are important.

Bismuth (Bi) has a high density, which allows it to effectively absorb and attenuate gamma radiation [31,32]. With a density of around 9.78 g/cm^3, it provides significant mass per unit volume, making it effective at blocking radiation [33]. Unlike lead, which has been traditionally used for radiation shielding but is toxic, Bi is considered safer for handling [34,35]. It has low toxicity levels, making it more environmentally friendly and suitable for applications where exposure to the shielding material is a concern [36–38]. Bi is stable and does not undergo significant radioactive decay itself [39]. This means that its shielding properties remain consistent over time, providing reliable protection against gamma radiation.

Herein, the present work uniquely involves the synthesis of chromium-bismuth nanocomposites using an environmentally friendly approach for the first time. The Cr_2O_3/Bi_2O_3 NCs are procured through an innovative green synthesis approach using Aloe vera as a reducing agent through a solution combustion technique. The synthesized NCs are characterized to assess their crystallographic, morphology, structure, and interaction properties through PXRD, SEM, EDS, FTIR, and UV–Vis spectroscopic techniques. Further, the obtained NCs in a pellet form are subjected to gamma irradiation and the radiation shielding properties are studied. The shielding parameters such as mass attenuation coefficient, half-value layer (HVL), tenth-value layer (TVL), mean free path (λ), energy buildup factor (EBF), and radiation protection efficiency (RPE) are calculated. Thus, the current study explores the effectiveness of Cr_2O_3/Bi_2O_3 NCs in gamma radiation shielding as a superior and sustainable alternative to traditional shielding materials.

2. Materials and methods

2.1. Preparation of Aloe vera gel extract

The Aloe vera leaves were harvested from the plant and thoroughly washed with tap running water followed by double-distilled water. The base of the leaves was trimmed, and the outer green layer was carefully removed using a clean knife that had been washed with double distilled water. The gel was then scooped out using a spoon and collected in a beaker for further use.

2.2. Green synthesis of the Cr_2O_3/Bi_2O_3 (1:1) NCs

The green synthesis of the Cr_2O_3/Bi_2O_3 (1:1) NCs are prepared by taking the stoichiometric ratio of Cr $(NO_3)_3{\cdot}9H_2O$ and Bi $(NO_3)_3{\cdot}5H_2O$ in a beaker. Fresh Aloe vera leaves are taken and outer skin is peeled to get its gel. The obtained gel is grinded in a mixer to get an even consistency. The as-prepared 30 ml of Aleo vera gel as a combustion fuel is added into the mixture and stirred vigorously using a magnetic stirrer for 15 min to get a uniform mixture of all the nitrates. Then, the obtained sample is kept in a pre-heated muffle furnace at 500 ± 10 °C for 10 min. The obtained product is grinded and calcinated for 3 h. The pinkish-cream Cr_2O_3/Bi_2O_3 nanocomposite crystals are obtained. The complete process is illustrated in a Fig. 1.

2.3. Characterization techniques

This study utilized various analytical techniques, including Powder X-ray Diffraction (PXRD) with Cu Kalpha radiation on a PANalytical X'Pert-PRO MPD instrument, Scanning Electron Microscopy (SEM) conducted with a Hitachi S-4200 instrument, UV absorption spectra recorded using a V-730 double-beam UV–Visible spectrometer, Fourier Transform Infrared Spectroscopy performed with a Perkin Elmer L1280134 instrument. The intensity of gamma radiation was measured using a gamma ray spectrometer, alongside the experimental setup as discussed in our previous studies [40].

3. Results and discussion

3.1. PXRD analysis

To know the phase purity of the synthesized nanocomposite (NCs) and its crystal structure, PXRD analysis was carried out. In PXRD pattern, the Bragg reflections observed at 27.1, 28.3, 29.02, 30.15, 31.27, 37.04, 45.54, 47.47, 53.35 and 53.94° 2θ values corresponds to (1 1 1), (1 2 0), (0 0 2), (2 2 0), (1 3 0), (0 2 3), (1 4 0), (−3 2 1) and (−2 4 1) planes. Bi_2O_3 crystallizes in monoclinic crystal structure. The planes match well with the JCPDS card no: 71-2274 [41]. The Bragg reflections observed at 34.80, 36.24, 43.94, 51.16, 56.31 and 57.90° 2θ values corresponds to (1 0 4), (1 1 0), (1 1 3), (0 2 4), (1 1 6) and (0 1 8) planes of Cr_2O_3. Cr_2O_3 crystallizes in rhombohedral crystal structure having space group R-3c (JCPDS card No. 38-1479) [42]. No other impurity related peaks were observed. The PXRD pattern of Cr_2O_3/Bi_2O_3 NCs is compared with the PXRD pattern of individual metal oxides. By considering the (1 1 1) plane, the crystallite size is calculated using Scherrer's formula [43]:

$$D_{hkl} = \frac{0.9\lambda}{cos\theta\beta_{hkl}} \quad (1)$$

where D, K, λ, β and θ stand for the size of the crystallite, Scherrer's constant (K = 0.9), the X-ray beam's wavelength, full width half maximum (FWHM), and Bragg angle respectively. The intercept and slope drawn between βcosθ v/s 4sinθ gives the crystallite size and lattice strain (Fig. 2b). The W-H plot method equation can be written as [44]:

$$\beta cos\theta = \epsilon(4sin\theta) + \frac{\lambda}{D} \quad (2)$$

where, β, ∈, θ, λ and D corresponds to FWHM, strain, Bragg angle, X-ray wavelength and crystallite size respectively. The crystallite size and other structural parameters such as dislocation density (δ) and stacking fault (SF) is determined by using the relation:

$$\delta = \frac{1}{D^2} \quad (3)$$

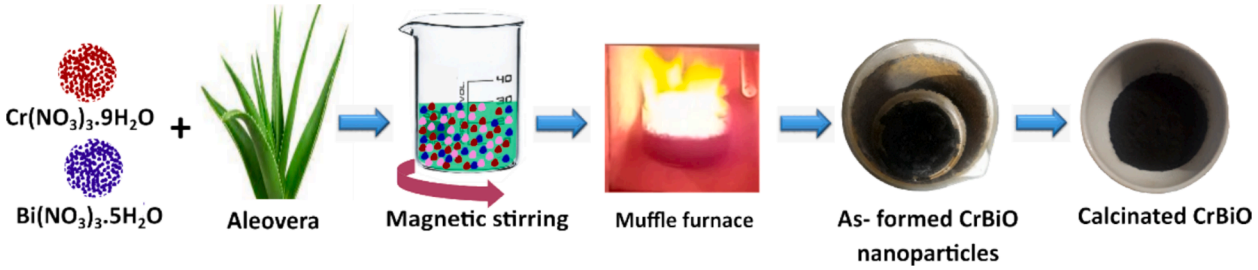

Fig. 1. Flowchart of synthesis of Cr_2O_3/Bi_2O_3 NCs.

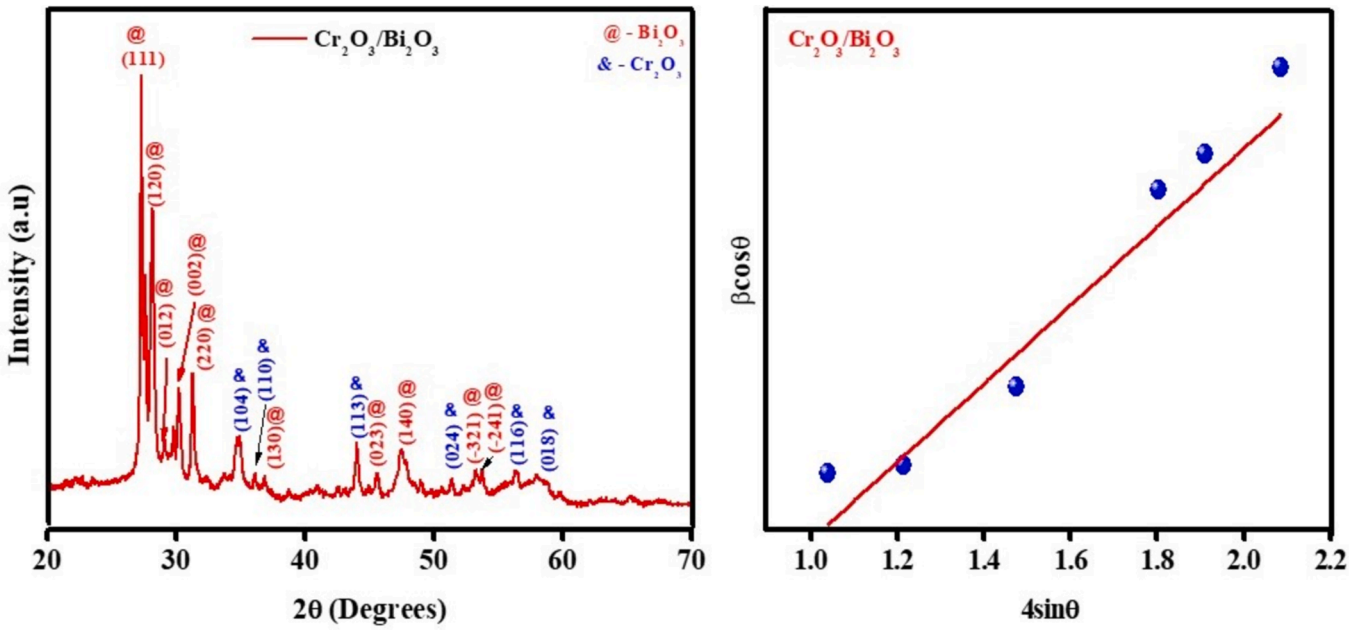

Fig. 2. (a) PXRD pattern and (b) W-H plot of Cr_2O_3/Bi_2O_3 NCs.

$$SF = \frac{2\pi^2}{45(3\tan\theta)^{\frac{1}{2}}} \quad (4)$$

$$\text{Crystallinity}\,(\%) = \frac{Area\ of\ the\ crystalline\ peaks}{Total\ area\ of\ the\ peaks} * 100 \quad (5)$$

The calculated crystallite size, strain, crystallinity, dislocation density and stacking fault are found to be 15 and 16.2 nm from Scherrer's and W-H plot method respectively, 3.781×10^{-3}, 89 %, 4.44×10^{15} line/m^2, and 0.4213 respectively.

4. B. SEM analysis

To know the surface morphology of the synthesized NCs, SEM analysis was carried out. Fig. 3(a–c) shows the SEM images of Cr_2O_3/Bi_2O_3 NCs at different magnification. The surface morphology of Cr_2O_3/Bi_2O_3 NCs consists large number of irregular shaped NCs. Among them few of them are smaller in size and a few of them are bigger in size. During combustion synthesis, rapid and intense heat is generated, leading to the evaporation and subsequent condensation of precursor materials. Gases released during combustion can create voids or cavities within the nanoparticles as they escape, leaving behind a hollow structure. The hollows observed on the surface are the characteristic of the combustion method. Fig. 3d represents the EDS spectra, which clearly indicates the presence of only Cr, Bi and O elements and also the absence of other impurities. The atomic and weight percentage of the elements present in the synthesized sample is given in inset of Fig. 3d.

4.1. FTIR analysis

The recorded FTIR spectra for Cr_2O_3/Bi_2O_3 nanocomposites (NCs) span the range of 4000—400 cm^{-1}. Various absorption peaks are discerned at specific wavenumbers, namely 511, 873, 1385, 1626, 2848, 2919, and 3409 cm^{-1}. The peak at 511 and 873 cm^{-1} is attributed to metal–oxygen (metal = Cr/Bi) stretching vibrations, while the presence of O–H bonds is indicated by the band at 3409 cm^{-1}. Additionally, the absorption peak at 1385 cm^{-1} is associated with −C-N vibrations. Another noteworthy IR absorption peak appears at 1626 cm^{-1} and is related to bending –OH vibrations. The IR absorption peak appeared at 2848 and 2919 cm^{-1} corresponds to alkyl stretching frequency [45] (see Fig. 4).

4.2. UV–visible absorption analysis and determination of energy band gap

The optical properties of the synthesized material were investigated through UV–Visible spectral analysis, aiming to elucidate its electronic transitions and determine the bandgap. Fig. 5 depicts the UV–Visible absorption spectrum of Cr_2O_3/Bi_2O_3 nanocomposites (NCs) within the wavelength range of 200–800 nm. Notably, a broad absorption spectrum spanning 300–400 nm is evident. In materials like Cr_2O_3/Bi_2O_3 NCs, diverse factors and physical processes contribute to such broad UV–Visible absorption spectra. Charge transfer transitions, involving the movement of electrons between distinct elements or ions within the compound, can significantly influence the absorption spectrum. Additionally, the presence of defects, impurities, or surface states may introduce extra energy levels, thereby contributing to the observed broad absorption spectrum.

Utilizing Tauc's plot, the optical bandgap of a material is determined by graphing $(\alpha h\nu)^2$ against photon energy ($h\nu$) to identify the bandgap energy. In the current investigation, the observed energy gap for Cr_2O_3/Bi_2O_3 NCs was determined to be 4.15 eV. Comparative studies indicate that the energy band gaps for Cr_2O_3 and Bi_2O_3 are reported as 3.2 eV [46] and 2.88 eV, respectively [47]. The combination of Cr_2O_3/Bi_2O_3 NCs leads to increase in the bandgap to 4.15 eV.

4.3. Gamma characteristics of Cr_2O_3/Bi_2O_3 NCs

The essential factors for evaluating shielding interaction comprise the linear attenuation coefficient, mass attenuation coefficient, HVL, TVL, λ, EBF, and RPE. The gamma radiation intensity was measured using a gamma ray spectrometer, with the experimental arrangement as shown in Fig. 6. The gamma ray spectrometer is composed of a NaI(Tl) scintillation detector system, a pre-amplifier, an amplifier, a cathode ray oscilloscope (CRO), a multi-channel analyzer (MCA), and a personal computer (PC).The spectrometer was first calibrated and its linearity was confirmed to calculate and analyse these parameters. By obtaining raw spectrum data from the NaI(Tl) detector, the gamma shielding parameters were calculated. The data recorded in the MCA clearly shows that gamma rays are absorbed in the sample. The emergent radiation intensities were quantified for 10,000 s, initially in the absence of any

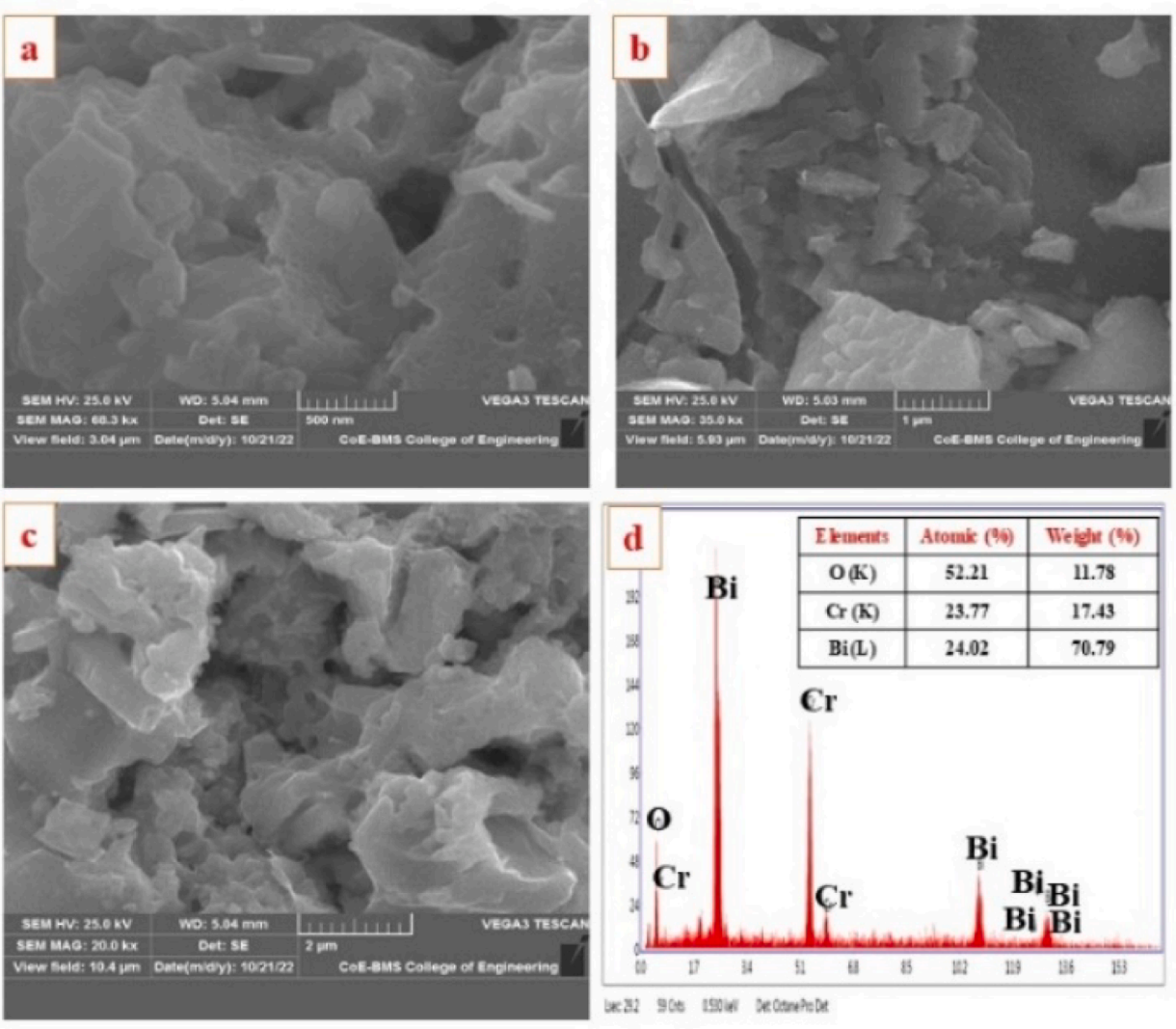

Fig. 3. (a–c) SEM image at different magnification, (d) EDS spectra (Inset: Atomic and weight percentage of elements) of Cr_2O_3/Bi_2O_3 NCs.

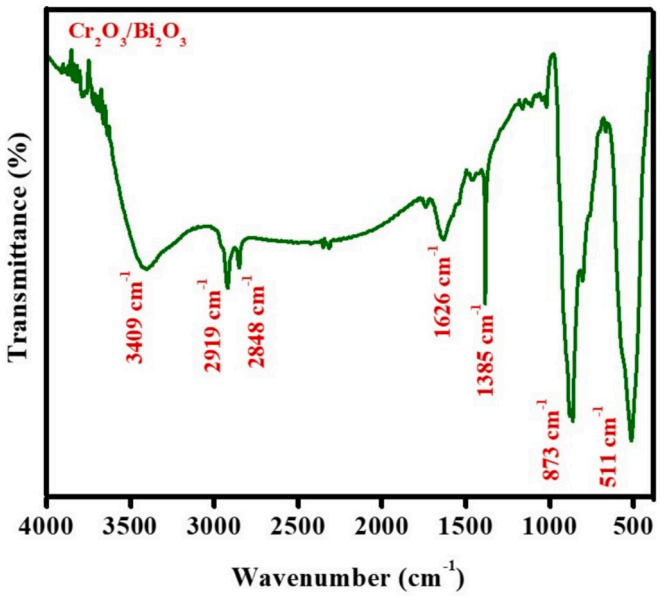

Fig. 4. FTIR spectra of Cr_2O_3/Bi_2O_3 NCs.

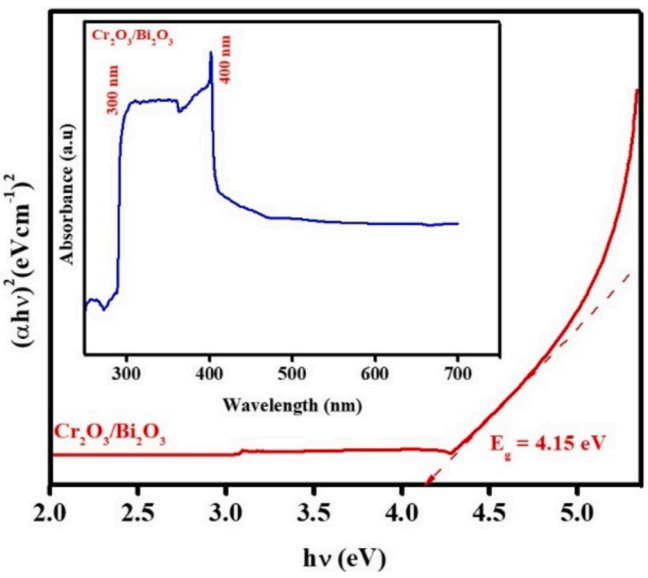

Fig. 5. Wood and Tauc's plot (UV–Visible absorption spectra) of Cr_2O_3/Bi_2O_3 NCs.

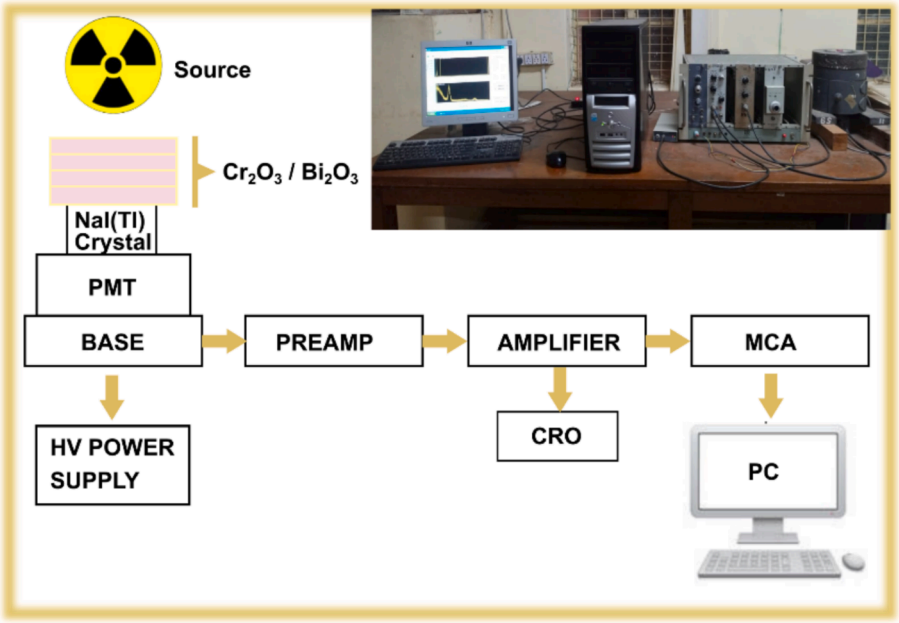

Fig. 6. Experimental setup for gamma shielding.

absorber and subsequently with Cr_2O_3/Bi_2O_3 NCs pellets employed as absorbers with varying thickness. The measurements included a range of energy spectra, including those corresponding to ^{22}Na, ^{137}Cs, and ^{60}Co.

Further, the mass attenuation coefficient of the sample is calculated using integral intensities and Beer Lambert's law [48]. Both the interaction energy and the material thickness affect the effectiveness of the shielding material. The mean free path is calculated as the inverse of the attenuation coefficient [49,50], which is influenced by the physical properties of the sample and the incident energy of photons. Specifically, in the case of high-energy photons, the mean free path increases as the energy of the photons increases, while it reduces with a rise in the atomic number of the material through which the photons traverse. Selecting a material that successfully lowers radiation intensity requires knowledge of its HVL and TVL values. The HVL is a key concept in radiation shielding, representing the thickness of a material required to reduce the intensity of radiation by 50 %. It is a crucial parameter in determining the shielding effectiveness of materials, as it directly correlates with how well the material can attenuate radiation. The HVL depends on both the type of radiation and the material used for shielding. For a given material, the lower HVL, more effective it is in attenuating radiation.

Furthermore, a comparison is made between the theoretical values and the experimental values of the shielding parameters which include μ/ρ, μ, HVL, TVL, and λ. The EDS composition of the Cr_2O_3/Bi_2O_3 NCs pellets was entered into the WinXCom software to obtain the theoretical values of the shielding parameters [51]. Table 1 shows both the experimental and theoretical values of shielding parameters at various energies. It is evident that there is good agreement between the experimental and theoretical shielding parameters. Furthermore, as shown in Fig. 7, it can be shown that an increase in source energy increased indicate HVL, TVL, λ and EBF, but a decrease in μ/ρ, μ, and RPE. These results visually indicates the effective shielding qualities of the synthesized Cr_2O_3/Bi_2O_3 NCs.

Table 1
Comparison of measured gamma shielding parameters with that of the theoretical values.

Source		^{22}Na	^{137}Cs	^{60}Co	
Energy (keV)		511	662	1173	1332
μ/ρ (cm^2/g)	Th	0.138	0.101	0.060	0.055
	Ex	0.120 ± 0.006	0.108 ± 0.005	0.058 ± 0.002	0.054 ± 0.002
μ (cm^{-1})	Th	0.057	0.041	0.025	0.023
	Ex	0.049 ± 0.002	0.044 ± 0.002	0.024 ± 0.001	0.022 ± 0.001
HVL (cm)	Th	12.09	16.52	27.44	29.95
	Ex	13.90 ± 0.695	15.44 ± 0.772	28.57 ± 1.428	30.64 ± 1.832
TVL (cm)	Th	40.18	54.90	91.20	99.55
	Ex	46.20 ± 2.310	51.34 ± 2.567	94.94 ± 4.747	101.8 ± 5.090
λ (cm)	Th	17.44	23.84	39.60	43.22
	Ex	20.06 ± 1.003	22.29 ± 1.114	41.23 ± 2.061	44.22 ± 2.211

5. Conclusion

This study presents a novel approach to gamma radiation shielding through the synthesis of Cr_2O_3/Bi_2O_3 NCs using a solution combustion method, with Aloe vera extract as a natural reducing agent. The characterization results supported the successful synthesis of the NCs revealing their crystallographic, surface, structural, and optical properties. The calculated crystallite size is found to be 15 nm from Scherrer's method and 16.2 nm from W-H plot. Also, strain, crystallinity, dislocation density and stacking fault calculated by PXRD analysis are found to be 3.781×10^{-3}, 89 %, 4.44×10^{15} line/m^2, and 0.4213 respectively. Surface analysis indicated nanoparticle aggregation with a flake-like structure. EDS spectrum analysis confirmed the presence of Cr, Bi, and O elements. The direct energy gap, determined from absorption spectra, was calculated as 4.15 eV. Further, evaluation of gamma radiation shielding capabilities indicated superior performance of Cr_2O_3/Bi_2O_3 NCs, as evidenced by the determined shielding parameters. The shielding parameters such as μ/ρ, μ, HVL, TVL and, λ are found to be 0.120, 0.108, 0.058 and 0.054 cm^2/g, 0.049, 0.044, 0.024 and 0.022 cm^{-1}, 13.90, 15.44, 28.57 and 30.64 cm, 46.20, 51.34, 94.94 and 101.8 cm and 20.06, 22.29, 41.23 and 44.22 cm at energies 0.511, 0.662, 1.173 and 1.332 MeV respectively. This research highlights the potential of Cr_2O_3/Bi_2O_3 NCs as a promising, environmentally friendly alternative to conventional radiation shielding materials.

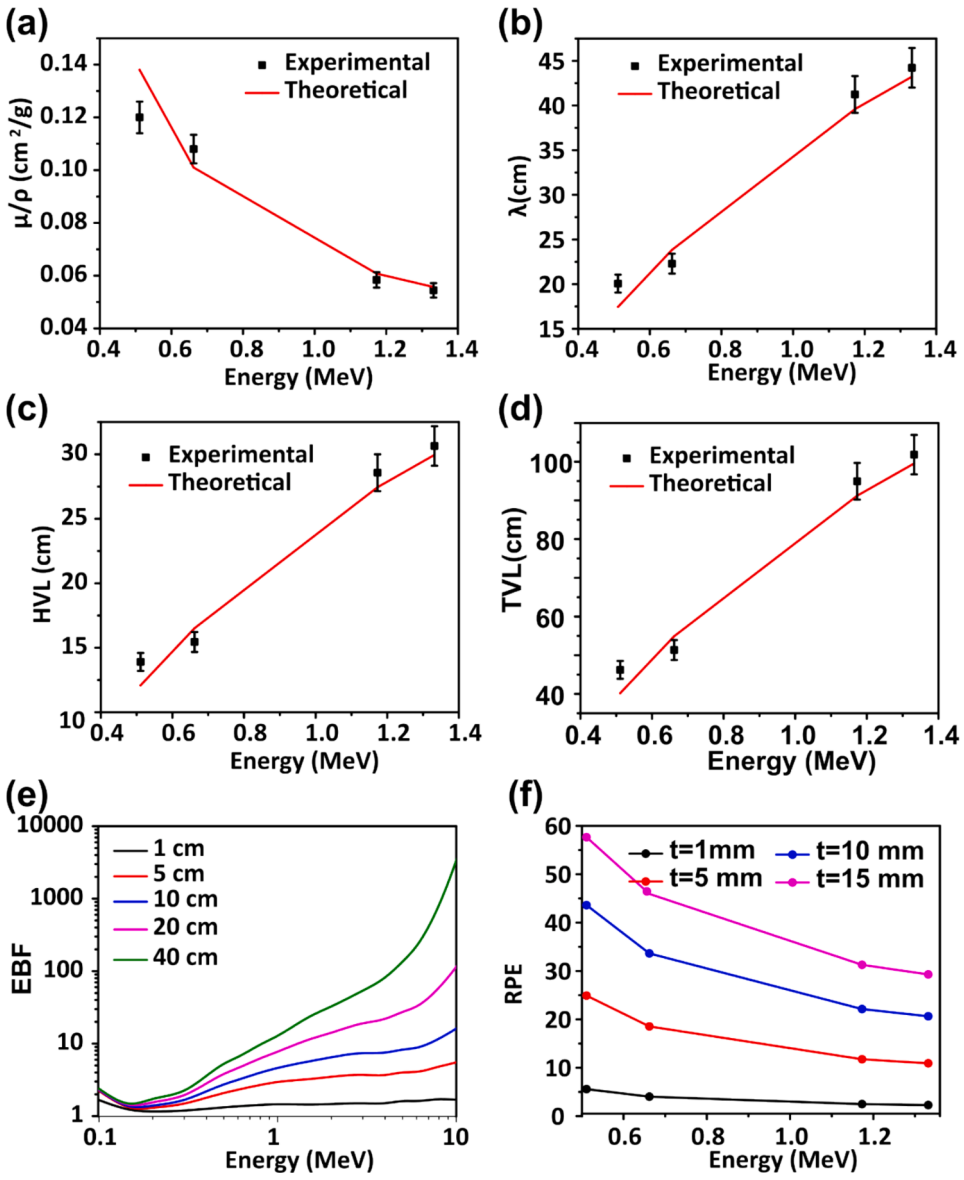

Fig. 7. Shielding parameters of Cr_2O_3/Bi_2O_3 NCs. (a) mass attenuation coefficient, (b) mean free path, (c) HVL, (d) TVL, (e) EBF, and (f) RPE.

CRediT authorship contribution statement

K. Kruthika: Conceptualization, Data curation, Formal analysis, Investigation, Methodology, Software, Validation, Visualization, Writing – original draft, Writing – review & editing. **S.M. Rumana Farheen:** Conceptualization, Validation, Writing – original draft, Writing – review & editing. **H.C. Manjunatha:** Supervision. **Y.S. Vidya:** Writing – original draft, Writing – review & editing. **K.N. Sridhar:** Writing – original draft, Writing – review & editing. **R. Munirathnam:** Writing – original draft, Writing – review & editing. **S. Manjunatha:** Software, Methodology. **S. Krishnaveni:** Supervision.

Declaration of competing interest

The authors declare that they have no known competing financial interests or personal relationships that could have appeared to influence the work reported in this paper.

Data availability

Data will be made available on request.

References

[1] A. C. E. S. CA, Independent research and development, 1999.
[2] H.M. Hashemian, Measurement of Dynamic Temperatures and Pressures in Nuclear Power Plants, The University of Western Ontario (Canada), 2011.
[3] Q. Chang, S. Guo, X. Zhang, Radiation shielding polymer composites: ray-interaction mechanism, structural design, manufacture and biomedical applications, Mater. Des. (2023) 112253.
[4] S. Olukotun, S. Gbenu, F. Ibitoye, O. Oladejo, H. Shittu, M. Fasasi, F. Balogun, Investigation of gamma radiation shielding capability of two clay materials, Nucl. Eng. Technol. 50 (2018) 957.
[5] A. Iqbal, P. Sambyal, C.M. Koo, 2d mxenes for electromagnetic shielding: a review, Adv. Funct. Mater. 30 (2020) 2000883.
[6] C.C. Ban, M.A. Khalaf, M. Ramli, N.M. Ahmed, M.S. Ahmad, A.M.A. Ali, E. T. Dawood, F. Ameri, Modern heavyweight concrete shielding: principles, industrial applications and future challenges; review, J. Build. Eng. 39 (2021) 102290.
[7] B. Aygün, High alloyed new stainless steel shielding material for gamma and fast neutron radiation, Nucl. Eng. Technol. 52 (2020) 647.
[8] M.N. Azman, N.J. Abualroos, K.A. Yaacob, R. Zainon, Feasibility of nanomaterial tungsten carbide as lead-free nanomaterial-based radiation shielding, Radiat. Phys. Chem. 202 (2023) 110492.
[9] S.J. Talley, T. Robison, A.M. Long, S.Y. Lee, Z. Brounstein, K.-S. Lee, D. Geller, E. Lum, A. Labouriau, Flexible 3d printed silicones for gamma and neutron radiation shielding, Radiat. Phys. Chem. 188 (2021) 109616.

[10] A. Acevedo-Del-Castillo, E.·Aguila-Toledo, S. Maldonado-Magnere, H. Aguilar-Bolados, A brief review on the high-energy electromagnetic radiation-shielding materials based on polymer nanocomposites, Int. J. Mol. Sci. 22 (2021) 9079.
[11] M.A.H. Abdullah, R.S.M. Rashid, M. Amran, F. Hejazii, N. Azreen, R. Fediuk, Y. L. Voo, N.I. Vatin, M.I. Idris, Recent trends in advanced radiation shielding concrete for construction of facilities: materials and properties, Polymers 14 (2022) 2830.
[12] H.M. Saleh, A.I. Hassan, Synthesis and characterization of nanomaterials for application in cost-effective electrochemical devices, Sustainability 15 (2023) 10891.
[13] K.N. Thakkar, S.S. Mhatre, R.Y. Parikh, Biological synthesis of metallic nanoparticles, Nanomed. Nanotechnol. Biol. Med. 6 (2010) 257.
[14] O.V. Kharissova, B.I. Kharisov, C.M. Oliva Gonźalez, Y.P. Ḿendez, I. Ĺopez, Greener synthesis of chemical compounds and materials, R. Soc. Open Sci. 6 (2019) 191378.
[15] J. Singh, T. Dutta, K.-H. Kim, M. Rawat, P. Samddar, P. Kumar, 'green' synthesis of metals and their oxide nanoparticles: applications for environmental remediation, J. Nanobiotechnol. 16 (2018) 1.
[16] U. Shanker, V. Jassal, M. Rani, B.S. Kaith, Towards green synthesis of nanoparticles: from bio-assisted sources to benign solvents. a review, Int. J. Environ. Anal. Chem. 96 (2016) 801.
[17] M. Rekha, M.P. Kumar, C. Srivastava, Electrochemical behaviour of chromium–graphene composite coating, RSC Adv. 6 (2016) 62083.
[18] A. Lousa, J. Romero, E. Martınez, J. Esteve, F. Montala, L. Carreras, Multilayered chromium/chromium nitride coatings for use in pressure die-casting, Surf. Coat. Technol. 146 (2001) 268.
[19] C. Hatchwell, N. Sammes, G. Tompsett, I. Brown, Chemical compatibility of chromium-based interconnect related materials with doped cerium oxide electrolyte, J. Eur. Ceram. Soc. 19 (1999) 1697.
[20] A. Elyahyaoui, K. Ellouzi, H.A. Zabadi, B. Razzouki, S. Bouhlassa, K. Azzaoui, E. M. Mejdoubi, O. Hamed, S. Jodeh, A. Lamhamdi, Adsorption of chromium (vi) on calcium phosphate: mechanisms and stability constants of surface complexes, Appl. Sci. 7 (2017) 222.
[21] U. Engstrom, D. Milligan, A. Klekovkin, Mechanical properties of high performance chromium materials, in: Advances in Powder Metallurgy and Particulate Materials, 2006, p. 07.
[22] C. Gonnelli, G. Renella, Chromium and nickel. Heavy Metals in Soils: Trace Metals and Metalloids in Soils and Their Bioavailability, 2013.
[23] A. Piotrowska, W. Pilch, L. Tota, G. Nowak, Biological significance of chromium iii for the human organism/biologiczne znaczenie chromu iii dla organizmu czlowieka, Medycyna Pracy 69 (2018) 211.
[24] J. Barnhart, Occurrences, uses, and properties of chromium, Regul. Toxicol. Pharm. 26 (1997) S3.
[25] A. Fetzer, M. Anger, P. Oleynik, J. Praks, Total ionising dose multilayer shielding optimisation for nanosatellites on geostationary transfer orbit, Adv. Space Res. 73 (2024) 831.
[26] S.U. Rahman, A.A. Ogwu, Corrosion and mott-schottky probe of chromium nitride coatings exposed to saline solution for engineering and biomedical applications, in: Advances in Medical and Surgical Engineering, Elsevier, 2020, pp. 239–265.
[27] K.C. Chan, Y. Harada, J. Liang, F. Yoshida, Deformation behaviour of chromium sheets in mechanical and laser bending, J. Mater. Process. Technol. 122 (2002) 272.
[28] Y. Liao, D. Raghu, B. Pal, L.A. Mielke, W. Shi, Cell counts: an r function for quantifying 10x chromium single-cell rna sequencing data, Bioinformatics 39 (2023) btad439.
[29] S. Sathya, V. Ragul, V.P. Veeraraghavan, L. Singh, M.N. Ahamed, An in vitro study on hexavalent chromium [cr (vi)] remediation using iron oxide nanoparticles based beads, Environ. Nanotechnol. Monit. Manage. 14 (2020) 100333.
[30] G. Genchi, G. Lauria, A. Catalano, A. Carocci, M.S. Sinicropi, The double face of metals: the intriguing case of chromium, Appl. Sci. 11 (2021) 638.
[31] B.C. Reddy, H. Manjunatha, Y. Vidya, K. Sridhar, U.M. Pasha, L. Seenappa, B. Sadashivamurthy, N. Dhananjaya, K. Sathish, P.D. Gupta, X-ray/gamma ray radiation shielding properties of α-Bi_2O_3 synthesized by low temperature solution combustion method, Nucl. Eng. Technol. 54 (2022) 1062.
[32] M. Sayyed, K.M. Kaky, M. Mhareb, A.H. Abdalsalam, N. Almousa, G. Shkoukani, M. A. Bourham, Borate multicomponent of bismuth rich glasses for gamma radiation shielding application, Radiat. Phys. Chem. 161 (2019) 77.
[33] F. Bakri, P.L. Gareso, D. Tahir, Advancing radiation shielding: a review the role of in x-ray protection, Radiat. Phys. Chem. (2024) 111510.
[34] A. Mostafa, H.M. Zakaly, M. Pyshkina, S.A. Issa, H. Tekin, H. Sidek, K. Matori, M. Zaid, Multi-objective optimization strategies for radiation shielding performance of bzbb glasses using Bi_2O_3: A fluka Monte Carlo code calculations, J. Mater. Res. Technol. 9 (2020) 12335.
[35] M.-A. Shahbazi, L. Faghfouri, M.P. Ferreira, P. Figueiredo, H. Maleki, F. Sefat, J. Hirvonen, H.A. Santos, The versatile biomedical applications of bismuth-based nanoparticles and composites: therapeutic, diagnostic, biosensing, and regenerative properties, Chem. Soc. Rev. 49 (2020) 1253.
[36] H.A. Maghrabi, A. Vijayan, P. Deb, L. Wang, Bismuth oxide-coated fabrics for x-ray shielding, Text. Res. J. 86 (2016) 649.
[37] S. Kaewpirom, K. Chousangsuntorn, S. Boonsang, Evaluation of micro-and nano-bismuth (iii) oxide coated fabric for environmentally friendly x-ray shielding materials, ACS Omega 7 (2022) 28248.
[38] N.J. AbuAlRoos, N.A.B. Amin, R. Zainon, Conventional and new lead-free radiation shielding materials for radiation protection in nuclear medicine: a review, Radiat. Phys. Chem. 165 (2019) 108439.
[39] P. De Marcillac, N. Coron, G. Dambier, J. Leblanc, J.-P. Moalic, Experimental detection of α-particles from the radioactive decay of natural bismuth, Nature 422 (2003) 876.
[40] B.C. Reddy, H. Manjunatha, Y. Vidya, K. Sridhar, U.M. Pasha, L. Seenappa, C. Mahen-drakumar, B. Sadashivamurthy, N. Dhananjaya, B. Sankarshan, et al., Synthesis and charac- terization of multi functional nickel ferrite nano-particles for x-ray/gamma radiation shielding, display and antimicrobial applications, Journalof Physics and Chemistry of Solids 159 (2021) 110260.
[41] V.K. Patel, R. Kant, M. Painuly, S. Bhattacharya, et al., Performance characterization of Bi_2O_3/Al nanoenergetics blasted micro-forming system, Defence Technol. 15 (2019) 98.
[42] S. Ponmudi, R. Sivakumar, C. Sanjeeviraja, C. Gopalakrishnan, T. Okamoto, Development of room temperature sensor based on high quality rhombohedral Al_2O_3: Cr_2O_3 (1: 1) thin film with bone like morphological feature for ultrasensitive detection of nh 3 gas, J. Mater. Sci. Mater. Electron. 31 (2020) 10123.
[43] R. Soundar, H. Manjunatha, Y. Vidya, R. Munirathnam, K. Sasidhar, L. Seenappa, K. Srid-har, S. Manjunatha, E. Krishnakanth, Deep blue emission and latent finger print detection analysis of zinc gallate nanoparticles, Mater. Res. Bull. 174 (2024) 112701.
[44] R. UmashankaraRaja, Y. Vidya, H. Manjunatha, M. Priyanka, R. Munirathnam, K. Rajashekara, S. Manjunatha, E. Krishnakanth, Effect of nickel doping on magnetic and di- electric properties of orthorhombic calcium ferrite nanoparticles, Green Energy Resour. (2024) 100059.
[45] B.B. Kamble, M. Naikwade, K. Garadkar, R.B. Mane, K.K.K. Sharma, B.D. Ajalkar, S. N. Tayade, Ionic liquid assisted synthesis of chromium oxide (Cr_2O_3) nanoparticles and their application in glucose sensing, J. Mater. Sci. Mater. Electron. 30 (2019) 13984.
[46] M.M. Abdullah, F.M. Rajab, S.M. Al-Abbas, Structural and optical characterization of cr2o3 nanostructures: evaluation of its dielectric properties, AIP Adv. 4 (2014).
[47] A. Han, J. Sun, G.K. Chuah, S. Jaenicke, Enhanced p-cresol photodegradation over biobr/Bi_2O_3in the presence of rhodamine b, RSC Adv. 7 (2017) 145.
[48] M.S. Al-Buriahi, B.T. Tonguc, Mass attenuation coefficients, effective atomic numbers and electron densities of some contrast agents for computed tomography, Radiat. Phys. Chem. 166 (2020) 108507.
[49] Y. Rammah, A. Ali, R. El-Mallawany, F. El-Agawany, Fabrication, physical, optical characteristics and gamma-ray competence of novel bismo-borate glasses doped with Yb_2O_3 rare earth, Physica B: Condensed Matter 583 (2020) 412055.
[50] R. El-Mallawany, Radiation shielding properties of tellurite glasses, in: Tellurite Glass Smart Materials, Springer, 2018, pp. 17–27.
[51] M. Sayyed, M. Mhareb, B.C. S¸akar, K. Mahmoud, E. S¸akar, H.A. Thabit, K. M. Kaky, S. Baki, Experimental investigation of structural and radiation shielding features of Li_2O-Bao-ZnO-B_2O_3-Bi_2O_3 glass systems, Radiat. Phys. Chem. 218 (2024) 111640.

Kruthika K.: pursuing her Ph.D. in Physics at the Department of Studies in Physics, University of Mysore (UOM), Mysuru, India. She has obtained her M.Sc. from University of Mysore in the year 2016. Her research interests include the synthesis and characterization of nanoparticles and radiation shielding.

Dr. Rumana Farheen S.M.: She is currently working as a CSIR-Research Associate. Received her Ph.D. in Physics (2024) with DST-INSPIRE fellowship, at the Department of Studies in Physics, University of Mysore (UOM), Mysuru, India. She has secured first rank in M.Sc. and B.Sc. and received seven Gold medals from UOM. Her research interests include the synthesis of nanoparticles, fabrication of flexible triboelectric nano-generators, energy harvesting devices, self-powered sensors, photoluminescence, radiation shielding, and supercapacitors.

Dr. Manjunatha. H.C.: received Ph.D.in Physics from Bangalore University. Presently working as Associate Professor in the Department of Physics, Government College for Women, Kolar. He has around 289 publications at national and international level. Indian Association of Nuclear Chemists and Allied Scientists (IANCAS) conferred "Dr. Tarun Datta Memorial Young Scientist Award-2018" in the field of Nuclear and Radiochemistry. Indian society for Radiation Physics conferred "Nucleonix Award for Young scientist- 2013". IANCAS also conferred "Best research paper Award". Vision group of science and technology, Govt. of Karnataka conferred "Seed money to young scientist Award-2013".

Dr. Vidya Y.S. - received her Ph.D in Physics from Bangalore University. She has bagged five gold medals in Physics and secured first rank in M.Sc. She is presently serving as Assistant Professor and Head, Department of Physics, Lal Bahadur Shastri Government First Grade College, RT Nagar, Bangalore – 560032. Her academic achievements include 15 years of teaching experience. She is also served as a member of board of studies in the autonomous institutions. She served as the Project Scientist in National Aerospace Laboratory on Oceanography. Her enthusiasm has significantly contributed in developing novel nanomaterials for Display, Forensic applications, Wastewater treatment and Nuclear Physics. She has published more than 150 research papers in reputed international journals. She is one of the author of the "SMART PHYSICS". She is also serving as reviewer in many top ranked journals. She is a recipient of "Seed money to Young Scientist Award" by VGST, Government of Karnataka in 2014-15, and "Young Scientist Research Award" by Unnathi Research Foundation.

Dr. Sridhar K.N.: received Ph.D.in Physics from Bharathiar University, Coimbatore. Presently working as Assistant Professor in the Department of Physics, Government First Grade College, Malur. He has around 120 publications at national and international level. His research areas include prediction of projectile – target combinations for the synthesis of superheavy elements, radiation shielding, synthesis of nanoparticles, photoluminescence, and supercapacitors.

MunirathnamR. : pursuing Ph.D.in Physics from Bharathidasan University, Trichy. Presently working as Assistant Professor in the Department of Physics, SDC Frist Grade College, Kolar. He has 82 publications at national and international level. His research areas include, Material science, Synthesis of Nanoparticles, Energy storage applications, NLO, radiation shielding, photoluminescence, and supercapacitors.

Dr. Manjunatha S.: obtained his Master degree in Analytical Chemistry from Bangalore University, Bengaluru in the year 2010 and Ph.D. degree from Visveswaraya Techno logical University, Belagavi in the year 2018. He is a INUP Research fellow at Centre for Nanoscience and Engineering (CeNSE), Indian Institute of Science (IISc) Bengaluru from 2014 to 16. He is having ten years of teaching experience at various levels. Presently, he is working as an Assistant Profes sor in the Department of Chemistry, BMS College of Engi neering, Bengaluru. Research interests includes synthesis and characterization of nanomaterials, Photoluminescence, water treatment, electrochemistry and Biological studies of nanomaterials.

Dr. Krishnaveni S.: received her Ph.D. degree in Physics from the University of Mysore, Mysuru, India, in 2003. Presently, working as Professor and Chairperson at Department of Studies in Physics, University of Mysore, Mysuru. She is first ranker in M.Sc. with 4 gold medals and had been CSIR-SRF and CSIR-RA during her research period. Her research interests include Compton profile measurements, fabrication of semi-conductor devices and study of radiation effects on them, simulation of biomolecules using molecular dynamics, fabrication and characterization of self-powered devices such as tribo-electric nanogenerators.